Materials Chemistry and Physics 307 (2023) 128087

Contents lists available at ScienceDirect

Materials Chemistry and Physics

journal homepage: www.elsevier.com/locate/matchemphys

Facile and green synthesis of disordered mesoporous silica as biogenic filler for mixed-matrix membranes

Wahyu Kamal Setiawan [a,b], Kung-Yuh Chiang [b,*]

[a] Department of Agroindustrial Technology, Universitas Internasional Semen Indonesia, Indonesia, SIG Industrial Complex, Veteran Street, Gresik, East Java, 61122, Indonesia

[b] Graduate Institute of Environmental Engineering, National Central University, Taiwan, No. 300, Chung-Da Road., Chung-Li District, Tao-Yuan City, 32001, Taiwan

HIGHLIGHTS

- Mesoporous silica was synthesized using a facile and green sol-gel process.
- Gluconic acid was a worthy replacement for the existing acid catalysts.
- PVA, PVP, and starch had a role to enhance the surface area of particles.
- PVP could govern spherical shape of silica particles.
- PVA/PVP gave a similar effect with PVP but was accompanied by an excellent particle size distribution.

GRAPHICAL ABSTRACT

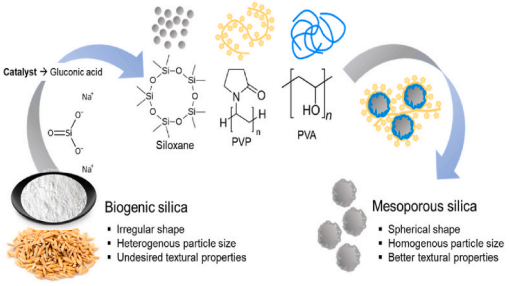

ARTICLE INFO

Keywords:
Eco-friendly approach
Sol-gel preparation
Nanoparticles
Disordered mesoporous silica
Rice husk

ABSTRACT

Disordered mesoporous silica particles (MSNs) were successfully synthesized using facile sol-gel using rice husk as a silica precursor and water-soluble polymers as structure-directing agents (SDAs) under acidic conditions of gluconic acid solutions. The influence of polyvinyl alcohol/PVA, polyvinylpyrrolidone/PVP, and soluble starch on the textural properties and morphologies were studied. Besides, the impact of MSNs with considerable properties on the CO_2/N_2 separation performance of poly(ether-*block*-amide) or Pebax membranes was also investigated. SDAs could generally double the specific surface area of the original sample up to 400–600 m^2/g, except PVP/starch and PVA/PVP. In addition, PVP governed spherical shape, while its combination with PVA established excellent particle size distribution (100–200 nm). MSNs prepared using PVA/PVP were even considered to upgrade Pebax membrane's CO_2/N_2 separation performance. CO_2 permeability and CO_2/N_2 selectivity were enhanced up to 58% and 21%, respectively, compared to pure Pebax membranes. This finding will be promising for encouraging sustainable filler development for membrane technology.

1. Introduction

Mesoporous silica nanoparticles (MSNs) are well-known valuable materials with several beneficial textural properties, excellent biocompatibility, and high flexibility toward surface modification [1,2]. As a result, it has received massive reliability for comprehensive applications such as solid-state sensors [3], biomedical materials [4], catalysts [5], aquatic pollutants removal [6], and gaseous pollutants

* Corresponding author.
E-mail address: kychiang@ncu.edu.tw (K.-Y. Chiang).

https://doi.org/10.1016/j.matchemphys.2023.128087
Received 30 December 2022; Received in revised form 16 June 2023; Accepted 18 June 2023
Available online 19 June 2023

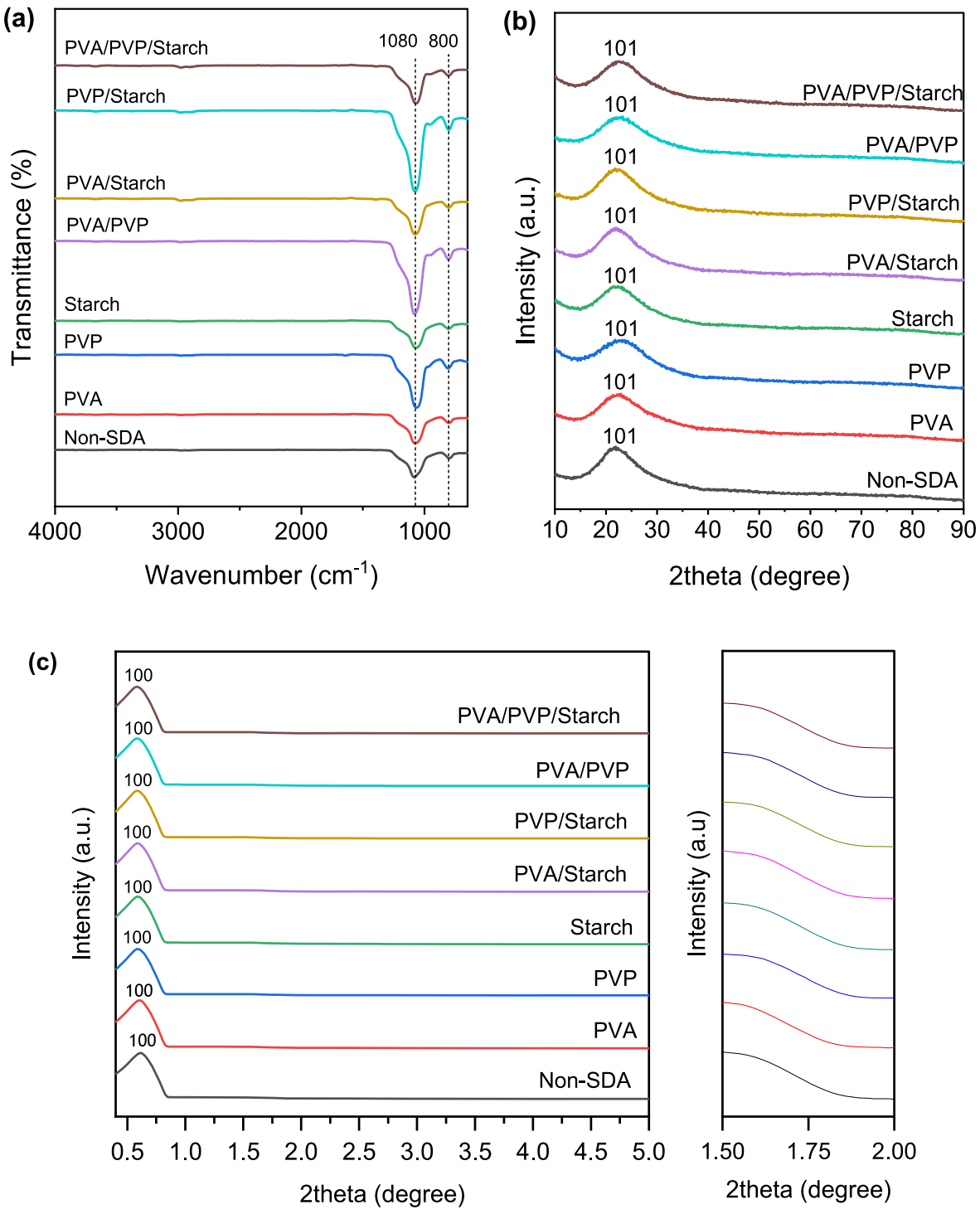

Fig. 1. FTIR spectra (a), wide-angle XRD pattern (b), and low-angle XRD pattern (c) of MSN with different structure-directing agents.

removal [7]. Moreover, the global mesoporous silica market is continuously growing and is predicted to value around USD 295.1 billion in 2027 [8]. Therefore, developing newly mesoporous silica with tunable properties is worth fulfilling the global market demand.

The Stober method recently prepared well-structured mesoporous silica [9–13]. However, it is challenging in large-scale production due to the utilization of high-cost silica precursors and the high-risk generation of harmful residues. Thus, seeking inexpensive and eco-friendly materials is necessary. As a result, waste-based materials from agricultural and industrial sectors, such as rice husk [14,15], bamboo leaf ash [16], banana peel ash [17], electronic waste [18], and ore tailings [19,20], were currently utilized as precursors to synthesize mesoporous silica. Likewise, less harmful acid catalysts were also used in the synthesis process, mostly from carboxylic acid families such as citric acid [21] and acetic acid [22]. In addition, the water-soluble templates might also be preferable to avoid the excessive employment of toxic solvents. Hwang et al. [22] used polyethylene glycol (PEG) as a morphology-directing agent to prepare mesoporous silica from sodium silicate. It was found that PEG exposed an ability to govern particle shape and mesopores arrangement. Another water-soluble polymer, polyvinyl alcohol (PVA), was reported by Thahir et al. [23] to synthesize the high surface area of mesoporous silica. While promising, several previous studies indicated

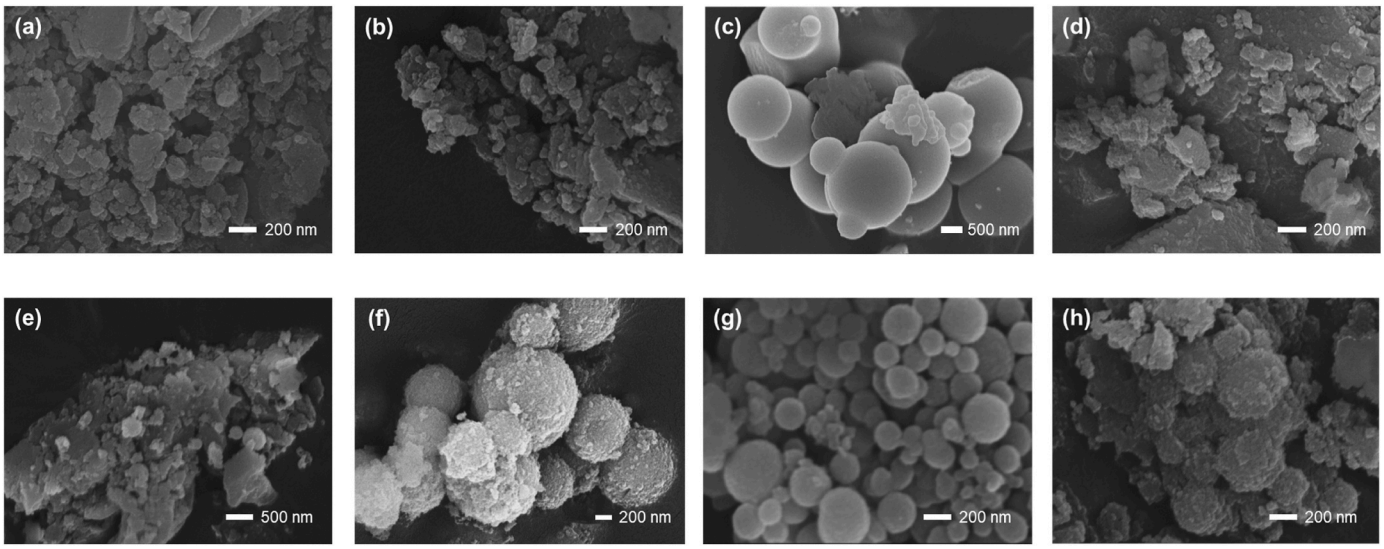

Fig. 2. SEM images of MSNs synthesized without SDA (a) and with PVA (b), PVP (c), starch (d), PVA/starch (e), PVP/starch (f), PVA/PVP (g), and PVA/PVP/starch (h).

that the applications of water-soluble polymers (e.g., starch and polyvinylpyrrolidone) in mesoporous silica synthesis were limited as a co-template along with the surfactant [24–27]. Thus, a further investigation of these materials is necessary to establish.

Employing filler materials from inexpensive and natural resources became a highly rated alternative to improve the gas separation performance of polymeric membranes [28]. For example, Bhattacharya and Mandal [29] have synthesized mesoporous silica derived from rice straw using precipitation. The silica sol was then incorporated into a polyether-polyamide block co-polymer matrix to obtain mixed matrix membranes. Waheed et al. [30] also employed an identical technique to generate rice husk-derived silica as a filler in polysulfone membrane for CO_2 separation. However, further studies would be necessary concerning poor dispersion between polymer-filler, causing overall membrane performance decrement.

This study developed a one-pot green synthesis of mesoporous silica for the first time by a sol-gel process using rice husk as a silica precursor and three different water-soluble polymer structure-directing agents (SDAs) under acidic conditions of gluconic acid solutions. Remarkably, the ability of polyvinyl alcohol (PVA), polyvinylpyrrolidone (PVP), and soluble starch to govern silica's pore structure and morphology was comparably studied. In addition, the potential of the best MSN for improving CO_2/N_2 separation features of poly(ether-*block*-amide) membranes was also investigated.

2. Materials and method

2.1. Materials

The rice husk was obtained from a local rice mill in Taoyuan City, Taiwan. D-gluconic acid ($C_6H_{12}O_7$ 50% aqueous solution) and soluble starch were acquired from Alfa Aesar. Sodium hydroxide (NaOH) was purchased from Showa Chemical. Polyvinyl alcohol (Mw = 89,000–98,000, PVA) and polyvinylpyrrolidone (Mw = 40,000, PVP) were supplied by Sigma Aldrich.

2.2. Mesoporous silica synthesis

Rice husk silica (RHS) was obtained by the process described elsewhere [31]. RHS and 2 mol L^{-1}, NaOH at a ratio of 1:10 (w/v), were refluxed to get a sodium silicate (Na_2SiO_3) solution. Mesoporous silica nanoparticle (MSNs) synthesis procedures were modified from another study [22]. Initially, 20 ml Na_2SiO_3 solution was mixed with 20 ml polymer solution (5% w/v). The weight ratio was controlled at the same level for the SDA mixtures. Next, gluconic acid was gradually added to adjust the pH to 4. The sol was then aged at 60 °C overnight. Finally, it was filtered and calcined at 550 °C for 2 h to obtain MSNs.

2.3. Membrane fabrication and gas permeation analysis

Dried Pebax pellets were dissolved into ethanol/water (70/30) at 70 °C for 2 h to obtain 4 wt% polymer solution. At the same time, the filler was separately dispersed into ethanol/water and sonicated at 25 °C for 2 h. The dispersed filler was mixed with polymer solution for another 2 h reflux process. Consequently, it was cast on a 6 mm PFTE circular dish and evaporated under ambient temperature for 48 h. Finally, the Pebax membrane was dried at 50 °C for 24 h under vacuum conditions. The single gas permeation of membranes was measured by custom permeation equipment at 25 °C and 1 bar operation. The single gas permeability, P (1 Barrer = 10^{-10} cm^3 STP $cm{\cdot}cm^{-2}s^{-1}cmHg^{-1}$) was determined using the following equation.

$$P = 10^{10}\frac{Q \times l}{\Delta P \times A}$$

Q is the permeate flow rate (cm^3/s STP), l is the membrane thickness (cm), A is the effective area (3.069 cm^2), and ΔP is the transmembrane partial pressure difference (cmHg). The ideal CO_2/N_2 selectivity was determined using the equation:

$$\alpha_{CO_2/N_2} = \frac{P_{CO_2}}{P_{N_2}}$$

where P_{CO2} and P_{N2} are the permeability of CO_2 and N_2, respectively.

2.4. Characterization methods

The wide-angle and low-angle X-ray diffraction (XRD) patterns of MSNs were characterized by XRD Bruker D8 Advance at 2θ = 10–90° and XRD D2 Phaser at 2θ = 0.4–10°, respectively. The MSNs surface properties were investigated using Fourier-transform Infrared (FTIR) Frontier at 650-4000 cm^{-1}. The Brunauer EmmetteTeller (BET) and Barrett-Joyner-Halenda (BJH) analyses were executed by nitrogen adsorption measurement using an Autosorb iQ instrument. The morphology of MSNs was observed using JEOL JSM-7600F Field Emission Scanning Electron Microscope (FESEM) and JEOL JEM-2100

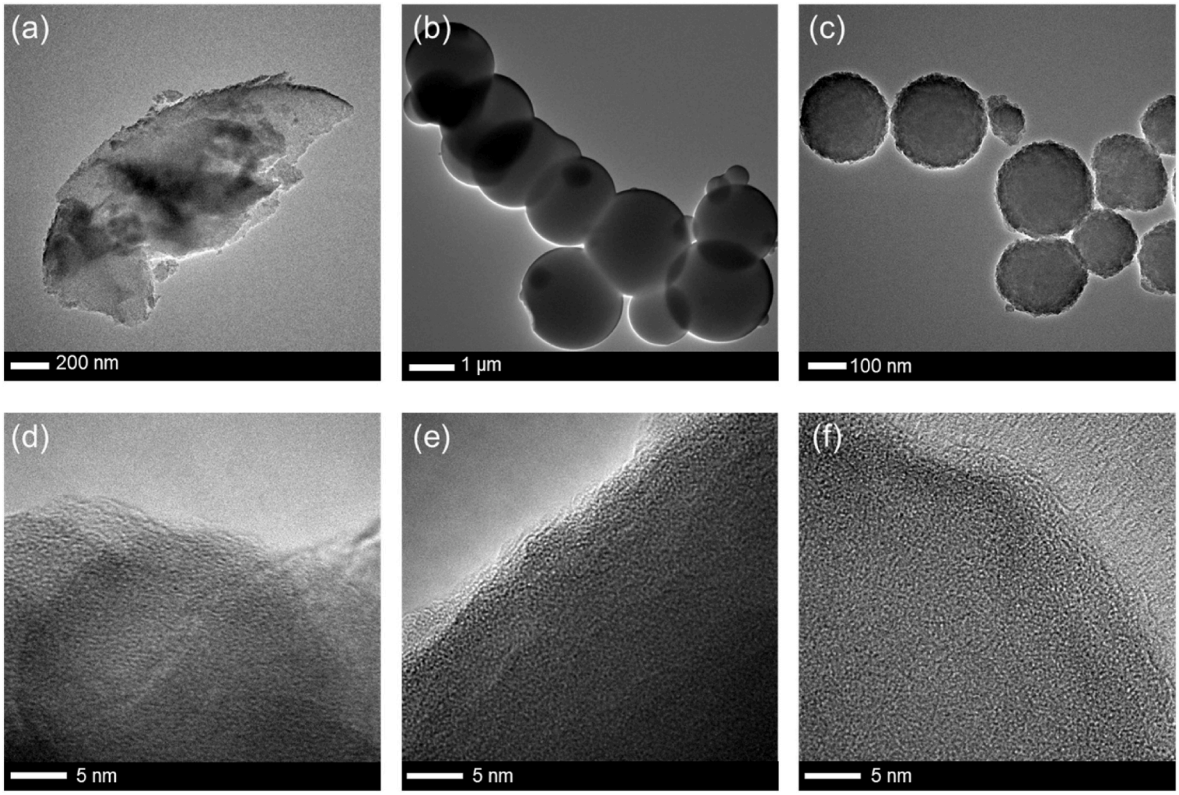

Fig. 3. TEM images of MSNs synthesized without SDA (a–d), with PVP (b–e), and with PVA/PVP (c–f).

Transmission Electron Microscope (TEM).

3. Results and discussion

FTIR analysis (Fig. 1a) indicated that all samples displayed identical spectra at around 1080 cm^{-1} and 800 cm^{-1}, ascribed to the asymmetric and symmetric stretching vibration of siloxane bonds ≡Si–O–Si≡, respectively [32]. The WAXRD analysis (Fig. 1b) revealed a broad peak at 2θ = 22° (1 0 1) for all MSNs, corresponding to amorphous silica nature. Moreover, the LAXRD pattern (Fig. 1c) showcased an intense (1 0 0) reflection at 2θ = 0.58° and a broad weak shoulder in the 2θ range 1.5°–2.0° for all MSNs samples, referring to wormholes pore

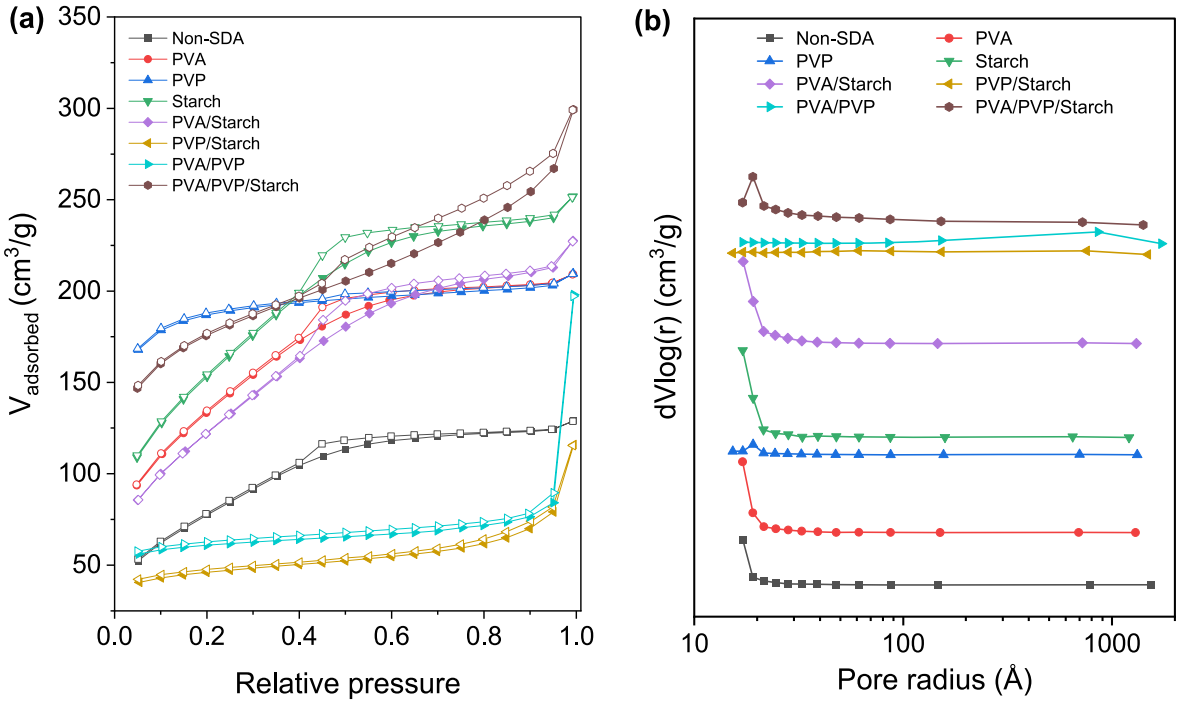

Fig. 4. The nitrogen adsorption/desorption isotherms (a) and pore size distribution (b) of MSN at different structure-directing agents.

Table 1
Textural properties of synthesized MSN with different structure directing agents.

Sample	Specific surface area (m^2/g)	Total pore volume (cm^3/g)	Average pore radius (Å)	BJH desorption summary		
				Pore surface area (m^2/g)	Pore volume (cm^3/g)	Pore radius (Å)
Non-SDA	293	0.20	13.7	57	0.063	17.1
PVA	486	0.32	13.3	96	0.100	17.0
PVP	574	0.32	11.3	23	0.036	19.1
Starch	553	0.39	14.1	131	0.145	17.1
PVA/Starch	451	0.35	15.6	139	0.165	17.1
PVP/Starch	146	0.18	24.5	28	0.114	17.1
PVA/PVP	298	0.43	28.9	30	0.287	15.3
PVA/PVP/ Starch	570	0.46	16.3	127	0.221	19.1

arrangement. Park and Pinnavaia [33] argued that these patterns indicated a correlated pore network distribution lacking a regular pore structure. Regarding FTIR and XRD results, it was then implied that the employment of PVA, PVP, starch, and their mixtures could not alter the pore framework of mesoporous silica.

SEM and TEM imaging were performed to assess the morphology of the prepared MSNs, as seen in Figs. 2 and 3. In the absence of SDAs, irregular shape and heterogenous particle size were observed. The employment of SDAs was expected to avoid particle aggregation and govern into uniform morphologies. PVA and starch, however, could not effectively configure the morphology despite the smaller particle size (see Fig. 2b and d). Moreover, their mixture was not even better with the aggregation phenomenon (Fig. 2e). In contrast, PVP became a better SDA concerning its ability to arrange micro-sized spherical particles of MSN with smooth surfaces (see Figs. 2c and 3b). The combination of PVP with other SDAs promoted rough surfaces with smaller particle sizes. Furthermore, PVP/PVA interestingly offered dispersed-spherical particles with uniform smaller particle sizes (100–200 nm), as illustrated in Figs. 2g and 3c. TEM images (Fig. 3d–f) were also beneficial to demonstrate the pore geometry of MSN. The wormhole-like pores were more visibly found on the outer surface of the MSN sample. It was because the inner part of pores was predominantly arranged by micro-sized gaps, which hindered the appearance of pore geometry.

Fig. 4a displays the nitrogen adsorption-desorption isotherms of MSN samples. All models exhibited type II closely related to type IV adsorption isotherm, confirming the mixture of micro-mesoporous structure. In addition, different hysteresis loops were observed, suggesting the existence of pores with non-identical pore shapes and sizes. Non-SDA MSNs showed a type-H4 hysteresis loop from $P/P_0 = 0.35$ to 0.75, indicating a limited amount of mesopores with slit-shape. Likewise, the PVA-MSN, PVP-MSN, Starch-MSN, PVA/Starch-MSN, and PVA/PVP/Starch-MSN showed an identical profile at $P/P_0 = 0.40$ to 0.99. Meanwhile, the PVP/Starch-MSN and PVA/PVP-MSN revealed a type-H3 hysteresis loop at $P/P_0 = 0.05$ to 0.99. Those indicated wedge-shaped pores with broad size distribution. Fig. 4b depicts the pore size distributions (PSD) calculated by the Barrett-Joyner-Halenda (BJH) model. Most MSN samples presented an identical unimodal distribution with a mean pore radius of 13.00–16.25 Å (see Fig. 4b and Table 1). Only PVP/Starch-MSN and PVA/PVP-MSN demonstrated a wide distribution with a larger mean pore radius at 24–29 Å.

BJH desorption results, as listed in Table 1, showed that single employment of SDA could significantly alter cumulative pore volume and surface area. PVA and starch positively impacted these pore properties, whereas PVP gave smaller values than non-SDA-MSN. The effect of PVP was also observed in the mixed SDAs (PVP/starch and PVA/PVP). The other SDA mixtures (PVA/starch and PVA/PVP/starch) likewise promote identical influences following their single dominant components. Furthermore, BET analysis implied that the presence of SDAs in the synthesis process could generally build up enormous narrow pores, elevating their specific surface area (400–600 m^2/g). On the contrary, PVP/starch and PVA/PVP presented relatively unchanged or even lower specific surface area (150–300 m^2/g) due to larger pore size with low

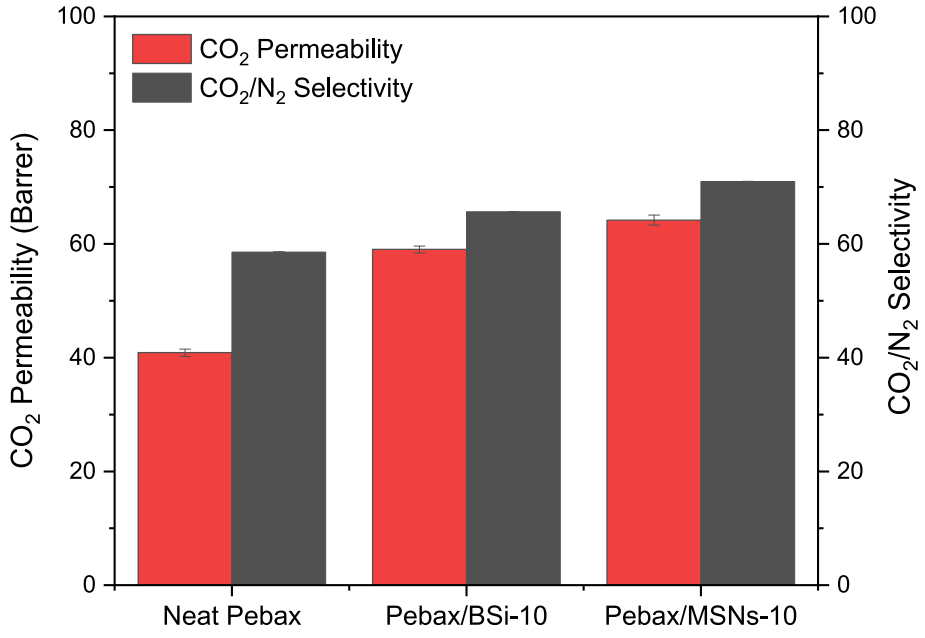

Fig. 5. CO_2/N_2 separation performance of Pebax mixed matrix membranes (MMMs) at 25 °C and 1 bar pressure.

occupancy.

Considering morphology, particle size distribution, and textural properties, mesoporous spherical biogenic silica nanoparticles (MSNs) prepared by PVA/PVP could be chosen as a filler to improve the CO_2/N_2 performance of Pebax membranes. MSNs exhibited a better impact on CO_2/N_2 separation features of Pebax membranes compared to original biogenic silica (BSi) from rice husk (as shown in Fig. 5). In particular, MSNs could homogenously spread out without severe tortuosity and have an excellent interfacial link-up within the polymer matrix. Hence, the appropriate pore aperture of MSNs (average pore size = 2.89 nm, as indicated in Table 1) could enable Knudsen diffusion transport for CO_2/N_2. As a result, Pebax membrane comprising 10 wt% MSNs exhibited 64.19 Barrer of CO_2 permeability (1.6 higher than pure Pebax) and CO_2/N_2 selectivity of 71 (1.2 higher than pure Pebax).

4. Conclusion

Disordered mesoporous silica was successfully synthesized by facile sol-gel process rice husk as a silica precursor and water-soluble polymers as structure-directing agents under acidic conditions of gluconic acid solutions. PVP could effectively control particle morphology into spherical shapes, whereas PVA and starch enhanced specific surface area. Moreover, PVA/PVP showed a remarkable particle size distribution without severe agglomeration. MSNs prepared using PVA/PVP exhibited more significant effect on CO_2/N_2 separation performance of Pebax membranes compared to original BSi. CO_2 permeability and CO_2/N_2 selectivity were upgraded to 58% and 21% by incorporating MSNs into Pebax membranes. This finding may incubate the development of biogenic filler in membrane technology for CO_2 separation.

CRediT authorship contribution statement

Wahyu Kamal Setiawan: Conceptualization, Writing – original draft, Writing – review & editing. **Kung-Yuh Chiang:** Methodology, Reviewing; Revising, Supervision.

Declaration of competing interest

The authors declare that they have no known competing financial interests or personal relationships that could have appeared to influence the work reported in this paper.

Data availability

The data that has been used is confidential.

Acknowledgment

The authors thank the Taiwan Ministry of Science and Technology (MOST) (Project No.: 109-2221-E-008-023-MY2) for financially supporting this work.

References

[1] C. Kim, S. Yoon, J.H. Lee, Facile large-scale synthesis of mesoporous silica nanoparticles at room temperature in a monophasic system with fine size control, Microporous Mesoporous Mater. 288 (2019), 109595, https://doi.org/10.1016/j.micromeso.2019.109595.

[2] Y. He, X. Hu, M. Xu, A.M.C. Ng, A.B. Djurišić, Mesoporous silica nanosphere-based oxygen scavengers, Microporous Mesoporous Mater. 327 (2021), 111426, https://doi.org/10.1016/j.micromeso.2021.111426.

[3] A. Pavoor Veedu, P. Deivasigamani, Chromoionophore integrated hexagonal mesopore silica monolith as reusable two-in-one solid-state sensor for the sequential optical recognition of ultra-trace Co^{2+} and Fe^{3+} ions, Microporous Mesoporous Mater. 343 (2022), 112139, https://doi.org/10.1016/j.micromeso.2022.112139.

[4] H. Long, W. Tian, S. Jiang, J. Zhao, J. Zhou, Q. He, Z. Tang, W. Shen, J. Wang, A dual drug delivery platform based on thermo-responsive polymeric micelle capped mesoporous silica nanoparticles for cancer therapy, Microporous Mesoporous Mater. 338 (2022), 111943, https://doi.org/10.1016/j.micromeso.2022.111943.

[5] L.-X. Zheng, B. Peng, J.-F. Zhou, B.-Q. Shan, Q.-S. Xue, K. Zhang, High efficient and stable thiol-modified dendritic mesoporous silica nanospheres supported gold catalysts for gas-phase selective oxidation of benzyl alcohol with ultra-long lifetime, Microporous Mesoporous Mater. 342 (2022), 112140, https://doi.org/10.1016/j.micromeso.2022.112140.

[6] W. Wang, X. Wu, J. Ji, S. Xu, D. Li, Y. Lin, Z. Chen, Z. Wu, L.-B. Sun, One-pot synthesis of Al-containing mesoporous silicas in a mildly acidic condition for efficient tetracycline adsorption, Microporous Mesoporous Mater. 346 (2022), 112300, https://doi.org/10.1016/j.micromeso.2022.112300.

[7] M.A. Hanif, N. Ibrahim, K. Md Isa, F. Muhammad Ridwan, T.A. Tuan Abdullah, A. A. Jalil, Tailoring the properties of calcium modified fibrous mesoporous silica KCC-1 for optimized sulfur dioxide removal, Microporous Mesoporous Mater. 330 (2022), 111610, https://doi.org/10.1016/j.micromeso.2021.111610.

[8] Grand View Research, Mesoporous Silica Market Size, Share & Trends Analysis Report by Product (SBA, MCM Series), by Application (Drug Delivery, Environmental Protection, Catalysis), by Region (APAC, North America), and Segment Forecasts, 2022, 2020 - 2027, https://www.grandviewresearch.com/industry-analysis/mesoporous-silica-market. (Accessed 9 November 2022), 2022.

[9] T. Haynes, O. Bougnouch, V. Dubois, S. Hermans, Preparation of mesoporous silica nanocapsules with a high specific surface area by hard and soft dual templating approach: application to biomass valorization catalysis, Microporous Mesoporous Mater. 306 (2020), 110400, https://doi.org/10.1016/j.micromeso.2020.110400.

[10] A. Ijaz, M.B. Yagci, C.W. Ow-Yang, A.L. Demirel, A. Mikó, Formation of mesoporous silica particles with hierarchical morphology, Microporous Mesoporous Mater. 303 (2020), 110240, https://doi.org/10.1016/j.micromeso.2020.110240.

[11] T.T.T. Ngo, E. Besson, E. Bloch, S. Bourrelly, R. Llewellyn, S. Gastaldi, P. L. Llewellyn, D. Gigmes, T.N.T. Phan, One-pot synthesis of organic polymer functionalized mesoporous silicas, Microporous Mesoporous Mater. 319 (2021), 111036, https://doi.org/10.1016/j.micromeso.2021.111036.

[12] J. Shao, Y. Zhao, D. Li, S. Xu, Z. Dou, Z. Sun, M. Cao, K. Fu, Y. Liu, Y. Zhou, Synthesis and characterization of superhydrophobic fluorinated mesoporous silica for oil/water separation, Microporous Mesoporous Mater. 344 (2022), 112240, https://doi.org/10.1016/j.micromeso.2022.112240.

[13] R. Muthusami, A. Kesavan, V. Ramachandran, V. Vasudevan, K. Irena, R. Rangappan, Synthesis of mesoporous silica nanoparticles with a lychee-like morphology and dual pore arrangement and its application towards biomimetic activity via functionalization with copper(II) complex, Microporous Mesoporous Mater. 294 (2020), 109910, https://doi.org/10.1016/j.micromeso.2019.109910.

[14] A. Mahdavi Fard, S. Askari, A. Afshar Ebrahimi, A. Heydarinasab, Green synthesis of SAPO-34 molecular sieve using rice husk ash as a silica source: evaluation of synthesis and catalytic performance parameters in methanol-to-olefin reaction, Microporous Mesoporous Mater. 341 (2022), 112037, https://doi.org/10.1016/j.micromeso.2022.112037.

[15] E. Elimbinzi, S.S. Nyandoro, E.B. Mubofu, J.C. Manayil, A.F. Lee, K. Wilson, Valorization of rice husk silica waste: organo-amine functionalized castor oil templated mesoporous silicas for biofuels synthesis, Microporous Mesoporous Mater. 294 (2020), 109868, https://doi.org/10.1016/j.micromeso.2019.109868.

[16] A. Arumugam, G. Karuppasamy, G.B. Jegadeesan, Synthesis of mesoporous materials from bamboo leaf ash and catalytic properties of immobilized lipase for hydrolysis of rubber seed oil, Mater. Lett. 225 (2018) 113–116, https://doi.org/10.1016/j.matlet.2018.04.122.

[17] D.F. Mohamad, N.S. Osman, M.K.H.M. Nazri, A.A. Mazlan, M.F. Hanafi, Y.A. M. Esa, M.I.I.M. Rafi, M.N. Zailani, N.N. Rahman, A.H.A. Rahman, N. Sapawe, Synthesis of mesoporous silica nanoparticle from banana peel ash for removal of phenol and methyl orange in aqueous solution, Mater. Today: Proc. 19 (2019) 1119–1125, https://doi.org/10.1016/j.matpr.2019.11.004.

[18] L.-Y. Lin, H. Bai, Facile and surfactant-free route to mesoporous silica-based adsorbents from TFT-LCD industrial waste powder for CO_2 capture, Microporous Mesoporous Mater. 170 (2013) 266–273, https://doi.org/10.1016/j.micromeso.2012.12.019.

[19] X. Han, Y. Wang, N. Zhang, J. Meng, Y. Li, J. Liang, Facile synthesis of mesoporous silica derived from iron ore tailings for efficient adsorption of methylene blue, Colloids Surf. A Physicochem. Eng. Asp. 617 (2021), 126391, https://doi.org/10.1016/j.colsurfa.2021.126391.

[20] C. Lu, H. Yang, J. Wang, Q. Tan, L. Fu, Utilization of iron tailings to prepare high-surface area mesoporous silica materials, Sci. Total Environ. 736 (2020), 139483, https://doi.org/10.1016/j.scitotenv.2020.139483.

[21] L. Li, D. Liu, Z. Guo, Y. Liu, W. Chu, Improved facile synthesis of mesoporous SBA-15-CTA using citric acid under mild conditions, J. Solid State Chem. 282 (2020), 121079, https://doi.org/10.1016/j.jssc.2019.121079.

[22] J. Hwang, J.H. Lee, J. Chun, Facile approach for the synthesis of spherical mesoporous silica nanoparticles from sodium silicate, Mater. Lett. 283 (2021), 128765, https://doi.org/10.1016/j.matlet.2020.128765.

[23] R. Thahir, A.W. Wahab, N.L. Nafie, I. Raya, Synthesis of high surface area mesoporous silica SBA-15 by adjusting hydrothermal treatment time and the, amount of polyvinyl alcohol 17 (1) (2019) 963–971, https://doi.org/10.1515/chem-2019-0106.

[24] C. Jin, Y. Guo, S. Zhang, W. Shen, Synthesis of large spherical mesoporous silica using tween-80 and starch hydrolysis solution, Adv. Sci. Lett. 5 (1) (2012) 204–207, https://doi.org/10.1166/asl.2012.1922.

[25] H. Liu, S. Ye, Y. Chen, Tailoring of pore size in mesoporous silica with stearic ACID and PVP, China Particuol. 3 (6) (2005) 379–382, https://doi.org/10.1016/S1672-2515(07)60218-8.

[26] M. Ulfa, K.S. Aristia, D. Prasetyoko, Synthesis of mesoporous silica materials via dual templating method from starch of waste rice and their application for drug delivery system, AIP Conf. Proc. 2049 (1) (2018), 020002, https://doi.org/10.1063/1.5082407.
[27] J. Zhang, G. Zhou, B. Jiang, M. Zhao, Y. Zhang, Effect of polyvinylpyrrolidone on mesoporous silica morphology and esterification of lauric acid with 1-butanol catalyzed by immobilized enzyme, J. Solid State Chem. 213 (2014) 210–217, https://doi.org/10.1016/j.jssc.2014.03.004.
[28] A.A. Ghazali, S. Abd Rahman, R. Abu Samah, Preparation and characterisation of pineapple peel waste as nanoadsorbent incorporated into Pebax 1657 nanocomposite membrane for CO2/CH4 separation, Mater. Today: Proc. 41 (2021) 88–95, https://doi.org/10.1016/j.matpr.2020.11.1012.
[29] W.K. Setiawan, K.-Y. Chiang, Eco-friendly rice husk pre-treatment for preparing biogenic silica: gluconic acid and citric acid comparative study, Chemosphere 279 (2021), 130541, https://doi.org/10.1016/j.chemosphere.2021.130541.
[30] M. Bhattacharya, M.K. Mandal, Synthesis of rice straw extracted nano-silica-composite membrane for CO2 separation, J. Clean. Prod. 186 (2018) 241–252, https://doi.org/10.1016/j.jclepro.2018.03.099.
[31] N. Waheed, A. Mushtaq, S. Tabassum, M.A. Gilani, A. Ilyas, F. Ashraf, Y. Jamal, M. R. Bilad, A.U. Khan, A.L. Khan, Mixed matrix membranes based on polysulfone and rice husk extracted silica for CO2 separation, Separ. Purif. Technol. 170 (2016) 122–129, https://doi.org/10.1016/j.seppur.2016.06.035.
[32] A. Marjani, R. Soltani, M. Pishnamazi, M. Rezakazemi, S. Shirazian, Functionalized pollen-like mesoporous silica, Microporous Mesoporous Mater. 310 (2021), 110531, https://doi.org/10.1016/j.micromeso.2020.110531.
[33] I. Park, T.J. Pinnavaia, Large-Pore Mesoporous Silica with Three-Dimensional Wormhole Framework Structures, (1387-1811 (Print)).